

Theoretical study of the valence $\pi \rightarrow \pi^*$ excited states of polyacenes: Benzene and naphthalene

T. Hashimoto, H. Nakano, and K. Hirao

Department of Applied Chemistry, Graduate School of Engineering, The University of Tokyo, Tokyo, Japan 113

(Received 25 September 1995; accepted 17 January 1996)

Multireference perturbation theory with complete active space self-consistent field (CASSCF) reference functions was applied to the study of the valence $\pi \rightarrow \pi^*$ excited states of benzene and naphthalene. The eigenvectors and eigenvalues of CASSCF with valence π active orbitals satisfy pairing properties for the alternant hydrocarbons to a good approximation. The excited states of polyacenes are classified into the covalent *minus* states and ionic *plus* states with the use of the alternancy symmetry. The present theory satisfactorily describes the ordering of low-lying valence $\pi \rightarrow \pi^*$ excited states. The overall accuracy of the present approach is surprisingly high. We were able to predict the valence excitation energies with an accuracy of 0.27 eV for singlet *u* states and of 0.52 eV or better for singlet *g* states of naphthalene. Our predicted triplet states spectrum provides a consistent assignment of the triplet–triplet absorption spectrum of naphthalene. For benzene we were able to predict the valence excitation energy with an accuracy of about 0.29 eV. The covalent *minus* states and ionic *plus* states exhibit different behavior as far as the electron correlation is concerned. The ionic *plus* states are dominated by the single excitations but covalent *minus* states include a large fraction of doubly excited configurations. The covalent *minus* states always give lower energy than the corresponding ionic *plus* states. This is true for triplet states. The dynamic σ – π polarization effects introduced by perturbation theory are significant for the ionic *plus* states while those on covalent excited states are usually of the same order as in the covalent ground state. The enlargement of the active space of the reference functions represents a great improvement of the description of the ionic states. The present approach with the pairing properties has proved to be of great value in understanding and predicting the experimental data of the alternant hydrocarbons. © 1996 American Institute of Physics. [S0021-9606(96)00216-6]

I. INTRODUCTION

The conjugate systems such as polyenes and polyacenes are deservedly the objects of a good deal of experimental and theoretical attention. The studies of the electronic structure of conjugated systems have a long history. The first and simplest form of the molecular orbital theory of conjugated molecules was proposed by Huckel in 1931.¹ Then, the idea was further developed by Goeppart-Mayer and Sklar,² Pariser and Parr,³ and Pople⁴ as π -electron theory for conjugated hydrocarbons. These simple but physical theories sometimes turn out to work much better than they *a priori* would be expected. The electronic structure of conjugated systems, particularly the optical spectra of polyacenes are surprisingly well described by Pariser–Parr–Pople (PPP) Hamiltonian.^{3,4} This is a model Hamiltonian, based primarily on the assumption of zero differential overlap. In the original version of the Pariser–Parr Hamiltonian only singly excited configurations were taken into account. Nevertheless, a great deal of understanding has been achieved on the interpretation of the optical spectra of hydrocarbons.

Benzene and naphthalene are alternant hydrocarbons, i.e., hydrocarbons containing no ring with an odd number of carbon atoms. For such systems, the Huckel and PPP Hamiltonians possess a special symmetry property usually referred to as the alternancy symmetry.^{4–7} The alternancy symmetry is closely related to the topological properties of the given

model. The apparent success of the PPP model to the spectra of alternant hydrocarbons seems to be mainly due to the alternancy symmetry properties. The other reason must be that the electron correlation effect, neglected in the approach, strongly affects mainly those singlet excited states which are dipole forbidden or weak and, hence, does not influence the main features of the calculated absorption spectra.⁸

The accurate *ab initio* treatment for such a large system as naphthalene has been limited so far. However, new development of *ab initio* molecular theory enables us to calculate such a large system quantitatively. Recently we have developed multireference based Rayleigh–Schrodinger perturbation theory, called multireference Møller–Plesset (MRMP) theory.⁹ The MRMP perturbation theory using the complete active space self-consistent field (CASSCF)¹⁰ reference function has been proved to be a useful method for obtaining reliable potential surfaces of chemical reactions and accurate transition energies for larger systems.^{11,12} In this paper, we will clarify the applicability of the multireference perturbation theory to the calculation of accurate excitation spectra of benzene and naphthalene. We also hope to investigate the general rules derived from the simple theories in view of the accurate *ab initio* theory.

In Sec. II we summarize the computational details. The alternancy symmetry and the classification of the states into *plus* and *minus* states are briefly discussed in order to under-

stand the basic features of the excited states of polyacenes in Sec. III. Calculated results and discussions of naphthalene and benzene are given in Secs. IV and V, respectively. Conclusions are presented in the final section.

II. COMPUTATIONAL DETAILS

The calculations were carried out for the ground and low-lying singlet and triplet $\pi \rightarrow \pi^*$ excited states of benzene and naphthalene. Experimental geometries¹³ were used, so the excitation energies calculated are vertical in nature. The molecules are placed in the xy plane with the long molecular axis corresponding to the x axis. Thus the dipole-allowed transitions of B_{3u} and B_{2u} in naphthalene are polarized along the long (x) and short (y) axes, respectively.

The basis sets used for carbon and hydrogen of benzene are Dunning's cc-pVTZ and cc-pVDZ,¹⁴ respectively. The Rydberg functions are not included in the present treatment. We have examined the effect of the polarization functions of H in benzene numerically and found that polarization functions on H have little effect on the valence $\pi \rightarrow \pi^*$ excitation energies. Computed excitation energies with $[4s3p2d/2s]$ are slightly larger by less than 0.03 eV than those with $[4s3p2d/2s1p]$ for both ionic and covalent states. The calculated oscillator strengths are almost the same with and without polarization on H. Thus for naphthalene, we used Dunning's cc-pVDZ for carbon and hydrogen but no polarization on H.

We first carried out the state-averaged CASSCF calculations. The active space should include all valence π orbitals in conjugated systems. For benzene, six π electrons were treated as active electrons and distributed among three bonding π and three antibonding π^* orbitals. In order to study the effect of the enlargement of the active space, we also used the extended active space, where 6 π electrons were distributed among 12 π orbitals. That is, the active space is doubled in each symmetry and the same set of calculations were performed. For naphthalene, ten π electrons are distributed among ten valence π orbitals.

Perturbation calculations were performed with the MRMP method. Thus the influence of the σ electrons is included in a perturbation treatment. The MRMP was applied to each individual state. Oscillator strengths were calculated by using transition moments computed at the CASSCF level and the MRMP transition energies.

III. ALTERNANCY SYMMETRY

First we shall briefly review the alternancy symmetry for the even alternant hydrocarbons in Huckel and PPP Hamiltonians. Let the valence π orbitals of the alternant hydrocarbons, which are normally filled in the ground state configuration, be designated by i, j, \dots , and those which are not filled by i', j', \dots . The occupied orbitals are numbered from the highest one down and the unoccupied orbitals from the lowest one up. The orbitals i and i' are called a conjugated pair and the well-known pairing properties are satisfied. These symmetry properties were first studied for Huckel Hamiltonians by Coulson and Rushbrooke⁵ and later for the PPP

Hamiltonians by Pople⁴ and others.^{6,7} These one-electron symmetry properties were first utilized by Pariser¹⁵ who distinguished the states as so-called "*plus*" and "*minus*" ones.

Now let us consider the low-lying singly excited configurations in even alternant hydrocarbons. Due to the well known relation of the π orbital energy, $\epsilon_i = -\epsilon_{i'} + \text{constant}$, the energy of the configuration obtained by exciting an electron from the π orbital i to the j' is equal to that obtained by excitation from j to i' , even with the inclusion of electronic interaction. The linear combinations of the two degenerate configurations generate the *minus* ($-$) and *plus* ($+$) states. The singly excited states are defined as follows

$$^1\Psi^\pm(ij') = |(ij' \pm i'j)(\alpha\beta - \beta\alpha)/2|,$$

$$^3\Psi^\pm(ij') = |(ij' \pm i'j)(\alpha\beta + \beta\alpha)/2|.$$

We used the abbreviation (ij') to represent a conjugated pair of one-electron transitions of $i \rightarrow j'$ and $j \rightarrow i'$. The choice of sign in the triplet wave functions is quite arbitrary. Our choice is *different* from the original Pariser's definition¹⁵ for triplet states but it is more useful to interpret the singlet and triplet excited states consistently. The *minus* state is antisymmetric and the *plus* state is symmetric, respectively, with respect to the interchanges of the conjugated pair of orbitals, $i \leftrightarrow i'$ and $j \leftrightarrow j'$. The *minus* state is a covalent state while the *plus* state is an ionic state both for singlet and triplet states, which stems from the character of the states in a valence bond description. The Hamiltonian matrix elements between singly excited configurations, $\Psi(ij')$ and $\Psi(kl')$ with $(ij') \neq (kl')$, are

$$\langle ^1\Psi^+(ij') | H | ^1\Psi^+(kl') \rangle = 4(ij' | kl') - (il | jk) - (ik | jl),$$

$$\begin{aligned} \langle ^1\Psi^-(ij') | H | ^1\Psi^-(kl') \rangle &= \langle ^3\Psi^+(ij') | H | ^3\Psi^+(kl') \rangle \\ &= (il | jk) - (ik | jl), \end{aligned}$$

$$\langle ^3\Psi^-(ij') | H | ^3\Psi^-(kl') \rangle = -(il | jk) - (ik | jl),$$

$$\langle ^1\Psi^-(ij') | H | ^1\Psi^+(kl') \rangle = \langle ^3\Psi^-(ij') | H | ^3\Psi^+(kl') \rangle = 0.$$

The *plus* states do not interact with the *minus* states. The ground state behaves like a *minus* state. The excited configurations of the type of $i \rightarrow i'$ behave like *plus* states for singlet spin states and *minus* states for triplet spin states. Thus the singlet state originated from the HOMO–LUMO transition is an ionic state but the corresponding triplet state is a covalent state. The doubly excited configurations of the type of $(i)^2 \rightarrow (j')^2$ behave like *minus* states. Thus the low-lying doubly excited state arising from the $(\text{HOMO})^2 \rightarrow (\text{LUMO})^2$ transition is predicted to interact with the singly excited $^1A_g^-$ states. The dipole transition moment between any two *plus* states or between any two *minus* states is zero. That is, only transitions between *plus* and *minus* states are allowed (all-*trans*-polyenes and polyacenes have a center of symmetry which gives rise to the following selection rules: $u \rightarrow u$ and $g \rightarrow g$ transitions are always one-photon forbidden whereas $u \rightarrow g$ and $g \rightarrow u$ transitions are two-photon forbidden). With the alternancy symmetry, one can write the energy of the singly excited states as

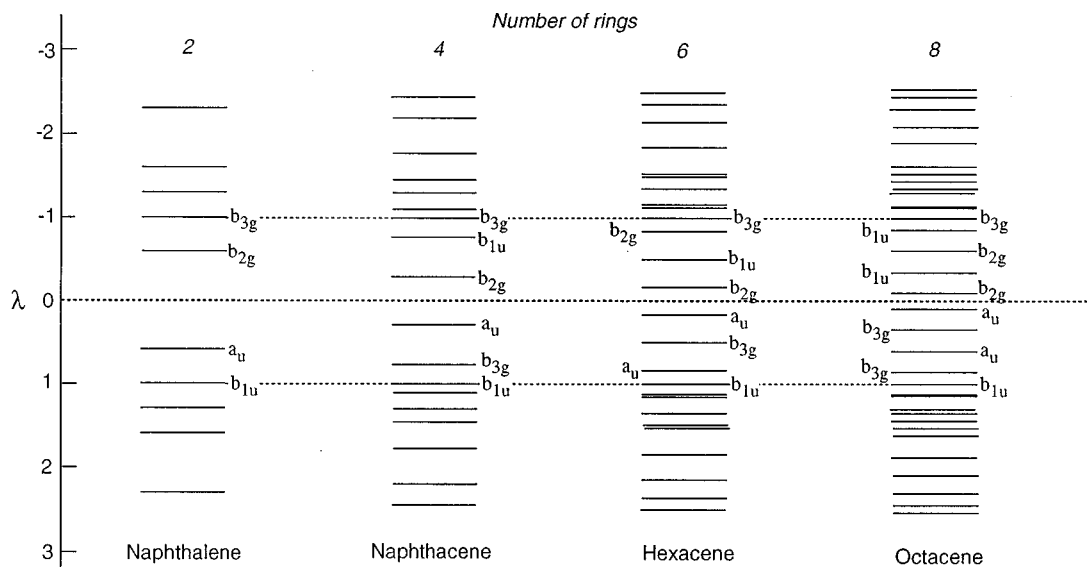


FIG. 1. The Huckel energy levels of π orbitals of small polyacenes with even number rings. The λ is a characteristic value of the Huckel secular equations.

$$\begin{aligned}
 E(^1\Psi^+(ij')) &= E_0 + \epsilon_{j'} - \epsilon_i + (ii|jj) \\
 &\quad + 3(ij'|ij') - (ij|ij), \\
 E(^1\Psi^-(ij')) &= E(^3\Psi^+(ij')) = E_0 + \epsilon_{j'} - \epsilon_i + (ii|jj) \\
 &\quad - (ij'|ij') + (ij|ij), \\
 E(^3\Psi^-(ij')) &= E_0 + \epsilon_{j'} - \epsilon_i + (ii|jj) \\
 &\quad - (ij'|ij') - (ij|ij),
 \end{aligned}$$

where E_0 is the doubly occupied ground state energy. The $(ii|jj)$ and $(ij|ij)$ are usual Coulomb and exchange integrals. Thus energies of the singlet *minus* and the corresponding triplet *plus* states are the same and we have the relations,

$$\begin{aligned}
 E(^1\Psi^-(ij')) &= E(^3\Psi^+(ij')) \geq E(^3\Psi^-(ij')), \\
 E(^1\Psi^+(ij')) &\geq E(^3\Psi^-(ij')).
 \end{aligned}$$

Note here that the above relations can only be satisfied within the CI with singles (CIS) approximation. Furthermore, the charge density of the ground state and all the singly excited states is 1 at each carbon atom.

Exact Huckel solutions of polyacenes were given by Coulson in 1948.¹⁶ The symmetry class of the conjugated pair of orbitals (i, i') is (a_u, b_{2g}) or (b_{1u}, b_{3g}) in D_{2h} symmetry orbitals. The corresponding symmetry class in benzene, which belongs to D_{6h} , is (a_{2u}, b_{3g}) or (e_{1g}, e_{2u}) . Therefore, the possible singly excited states arising from transitions from i to j' have the symmetry A_g, B_{1g}, B_{2u} , and B_{3u} in D_{2h} symmetry. The corresponding states in benzene are $A_{1g}, E_{2g}, B_{1u}, B_{2u}$, and E_{2u} in D_{6h} symmetry.

Figures 1 and 2 show the energy levels of π orbitals of small polyacenes obtained in Huckel approximation. There is a simple rule on the order of π orbitals. Let n be the number of rings in the polyacenes. When n is even, the symmetry to which the occupied orbitals belong is $a_u, b_{3g}, a_u, b_{3g}, \dots$ from the highest one down. The sequence of a_u and b_{3g}

continues until the $(n/2+1)$ orbital. The symmetry of the $(n/2+1)$ orbital is b_{1u} and its characteristic value λ of the Huckel secular equations is 1. For unoccupied orbitals, the symmetry class is $b_{2g}, b_{1u}, b_{2g}, b_{1u}, \dots$, from the lowest one up. The sequence also continues until the $(n/2+1)'$ orbital with $\lambda = -1$, which belongs to b_{3g} . When n is odd, the sequence of occupied orbitals of b_{3g}, a_u, \dots , also continues until the $(n+3)/2$ orbital. The $(n+3)/2$ orbital has b_{2g} symmetry and its orbital energy is degenerate with that of the $(n+1)/2$ orbital. The λ of these degenerate orbitals is equal to 1. The sequence of the unoccupied orbitals is b_{1u}, b_{2g}, \dots . The $(n+3)/2'$ orbital has a_u symmetry with $\lambda = -1$ and its orbital energy is also degenerate with that of the $(n+1)/2'$ orbital. For example, in benzene with $n=1$, the b_{2g} orbital with $\lambda=1$ is degenerate with b_{3g} HOMO and the a_u orbital with $\lambda=-1$ is degenerate with the b_{1u} LUMO.

The $i-i'$ excitations including the HOMO-LUMO transition always give $B_{2u}^+ (= a_u \times b_{2g} = b_{1u} \times b_{3g})$ symmetry for singlet spin states and B_{2u}^- symmetry for triplet spin states. The $^1B_{2u}^+$ and $^3B_{2u}^-$ states originating from single excitation from the occupied orbital with $\lambda=1$ to the unoccupied orbital with $\lambda=-1$ have the same energy for all the polyacenes in Huckel approximation.

The double excitation of $(\text{HOMO})^2 \rightarrow (\text{LUMO})^2$ gives $^1A_g^-$ symmetry. The $(\text{HOMO})^2 \rightarrow (\text{LUMO})(\text{LUMO}+1)$ and its conjugated transition give $^1,^3B_{1g}$ for small polyacenes ($n=1-3$) and $^1,^3B_{3u}$ for larger polyacenes ($n \geq 3$). These low-lying doubly excited states are expected to interact with the singly excited states with the same symmetry.

In the case of all-*trans*-polyenes, the symmetry class of the π orbitals i and its conjugate i' is (a_u, b_g) in C_{2h} symmetry. The HOMO and LUMO of all-*trans*-polyenes with odd number of double bonds (even number of double bonds) have the symmetry of $a_u(b_g)$ and $b_g(a_u)$, respectively. Therefore, the possible singly excited states from i to j' have the symmetry B_u and A_g in C_{2h} symmetry. The HOMO-

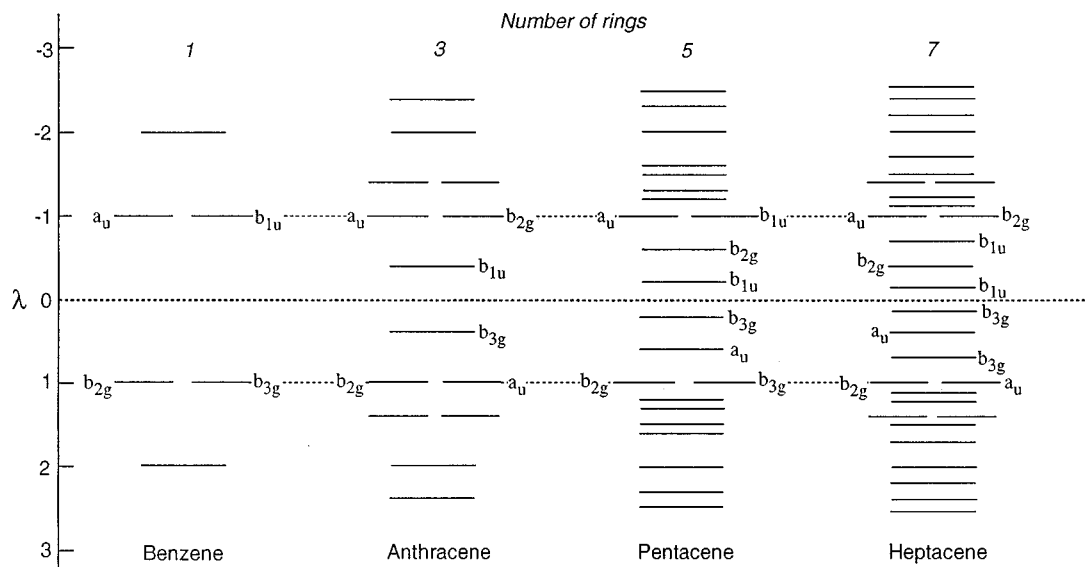


FIG. 2. The Huckel energy levels of π orbitals of small polyacenes with odd number rings. The λ is a characteristic value of the Huckel secular equations.

LUMO and other $i \rightarrow i'$ excitations always give B_u^+ symmetry for singlet spin states and B_u^- symmetry for triplet spin states. This is true even for the $\pi \rightarrow \pi^*$ excited state of ethylene. The singlet state of ethylene is an ionic ${}^1B_u^+$ (${}^1B_{1u}^+$ in D_{2h}) and the corresponding triplet state is a covalent ${}^3B_u^-$ (${}^3B_{1u}^-$) state. The double excitation of $(\text{HOMO})^2 \rightarrow (\text{LUMO})^2$ gives ${}^1A_g^-$ symmetry and the $(\text{HOMO})^2 \rightarrow (\text{LUMO})(\text{LUMO}+1)$ and its conjugated transition give ${}^{1,3}B_u$ symmetry. These low-lying doubly excited states are also expected to interact with the singly excited states with the same symmetry.

The general rules mentioned above are satisfied in the Huckel and PPP Hamiltonians but could possibly serve as a valuable tool for the qualitative interpretation of the excited states calculated with the sophisticated *ab initio* methods of alternant hydrocarbons and even of their substituted and heterocyclic analogues.

IV. LOW-LYING $\pi \rightarrow \pi^*$ EXCITED STATES OF NAPHTHALENE

Much effort has been devoted to the understanding of absorption spectra of naphthalene. Although benzene is a prototype of aromatic molecules, naphthalene is more interesting for spectroscopic studies. This is due to its lower symmetry which allows many transitions that are forbidden in benzene. The phosphorescence and some of the fluorescence of naphthalene appear in the visible region of the spectrum while emissions of benzene are located in the ultraviolet region. Naphthalene is thus probably the best experimentally examined polyacene.^{17–39} Thus, we first discuss the calculated results of naphthalene.

The CASSCF configurations for the ground and low-lying valence excited states are given in Table I. The ground state is well described by the Hartree–Fock configuration. The ground state is of a covalent character. The energy was computed to be $-384.616\,35$ a.u. at the MRMP level. Calcu-

lated vertical excitation energies and oscillator strengths with the experimental data available are summarized in Table II. Schematic summary of the singlet excitation energies is given in Fig. 3. Although previous *ab initio* calculations are limited, there are many semiempirical calculations^{8,30,40} of the spectrum of naphthalene following Pariser's pioneering work.¹⁵ The present results have been compared in Table III to the previous calculations: the semiempirical CIS by Pariser¹⁵ and Swiderek *et al.*³⁰ and the *ab initio* SAC-CI⁴¹ and the CASSCF plus second-order perturbation theory (CASPT2) by Rubio *et al.*⁴²

The ten valence π orbitals in naphthalene are in the order of energy: $1b_{1u}$, $1b_{2g}$, $1b_{3g}$, $2b_{1u}$, $1a_u$, $2b_{2g}$, $2b_{3g}$, $3b_{1u}$, $2a_u$, and $3b_{3g}$. The first five are occupied orbitals. They are designated by 5, 4, 3, 2, 1, $1'$, $2'$, $3'$, $4'$, and $5'$, respectively. The HOMO–LUMO ($1 \rightarrow 1'$) excitation gives rise to the lowest ${}^1B_{2u}^+$ state with the ionic nature. The two single excitations of $1 \rightarrow 2'$ and $2 \rightarrow 1'$ result in a pair of covalent ${}^1B_{3u}^-$ and ionic ${}^1B_{3u}^+$ states. Transitions to ${}^1B_{3u}^-$ states are pseudoparity forbidden while transitions to ${}^1B_{2u}^+$ and ${}^1B_{3u}^+$ states are dipole allowed. Transitions from 2 to $3'$ with its alternancy symmetry conjugate give dipole forbidden ${}^1A_g^-$ states. A double excitation of $(1)^2 \rightarrow (1')^2$ also gives rise to ${}^1A_g^-$ state, which is proposed to lie in this energy range. If such a state exists, it interacts with the singly excited ${}^1A_g^-$ states. Two single excitations of $1 \rightarrow 3'$ and $3 \rightarrow 1'$ give rise to a pair of covalent ${}^1B_{1g}^-$ and ionic ${}^1B_{1g}^+$ states. Similarly double excitations of $(1)^2 \rightarrow (1')(2')$ with its alternancy symmetry conjugate give ${}^1B_{1g}^-$ and ${}^1B_{1g}^+$ states in this energy range. The double excitations are expected to have a profound effect on the description of the dipole-forbidden ${}^1A_g^-$ and ${}^1B_{1g}^-$ states of naphthalene.

For triplet excited states, the HOMO–LUMO ($1 \rightarrow 1'$) excitation gives rise to the lowest ${}^3B_{2u}^-$ state with a covalent nature. The two single excitations of $1 \rightarrow 2'$ and $2 \rightarrow 1'$ result in a pair of covalent ${}^3B_{3u}^-$ and ionic ${}^3B_{3u}^+$ states. Transitions

TABLE I. Main configurations in CASSCF wave functions of naphthalene.^a

Singlet			Triplet		
State	Transitions	Coefficients	State	Transitions	Coefficients
$1^1A_g^-$	$(5)^2(4)^2(3)^2(2)^2(1)^2$	0.901	$1^3B_{3u}^-$	$1 \rightarrow 2'$	0.610
	$1 \rightarrow 1', 2 \rightarrow 2'$	-0.155		$2 \rightarrow 1'$	-0.588
	$1 \rightarrow 1', 3 \rightarrow 3'$	0.139		$3 \rightarrow 4'$	0.127
	$(1)^2 \rightarrow (1')^2$	-0.121		$4 \rightarrow 3'$	-0.142
$1^1B_{3u}^-$	$1 \rightarrow 2'$	0.593	$1^3B_{2u}^-$	$1 \rightarrow 1', 2 \rightarrow 4'$	0.131
	$2 \rightarrow 1'$	-0.601		$1 \rightarrow 1', 4 \rightarrow 2'$	-0.140
				$1 \rightarrow 1'$	0.772
$1^1B_{2u}^+$	$1 \rightarrow 1'$	0.869		$2 \rightarrow 2'$	0.347
	$2 \rightarrow 2'$	0.302		$3 \rightarrow 3'$	0.284
				$4 \rightarrow 4'$	0.166
$1^1B_{3u}^+$	$1 \rightarrow 2'$	0.621	$1^3B_{3u}^+$	$1 \rightarrow 2'$	0.672
	$2 \rightarrow 1'$	0.612		$2 \rightarrow 1'$	0.656
				$2 \rightarrow 3'$	0.455
$2^1A_g^-$	$2 \rightarrow 3'$	0.524	$1^3A_g^-$	$3 \rightarrow 2'$	-0.479
	$3 \rightarrow 2'$	-0.515		$1 \rightarrow 4'$	-0.351
	$1 \rightarrow 4'$	-0.128		$4 \rightarrow 1'$	0.450
	$4 \rightarrow 1'$	0.173			
	$(1)^2 \rightarrow (1')^2$	0.248	$1^3B_{1g}^-$	$1 \rightarrow 3'$	0.608
	$1 \rightarrow 1', 2 \rightarrow 2'$	0.208		$3 \rightarrow 1'$	-0.613
$1^1B_{1g}^-$	$1 \rightarrow 3'$	0.492		$2 \rightarrow 4'$	0.116
	$3 \rightarrow 1'$	-0.501		$4 \rightarrow 2'$	-0.143
	$1 \rightarrow 1', 1 \rightarrow 2'$	0.266			
	$1 \rightarrow 1', 2 \rightarrow 1'$	-0.300			
	$1 \rightarrow 3', 2 \rightarrow 3'$	0.147			
	$3 \rightarrow 1', 3 \rightarrow 2'$	-0.144			
$2^1B_{2u}^+$	$2 \rightarrow 2'$	0.831	$2^3B_{2u}^-$	$2 \rightarrow 2'$	0.789
	$1 \rightarrow 1'$	-0.225		$1 \rightarrow 1'$	0.346
	$3 \rightarrow 3'$	0.254		$2 \rightarrow 2', 1 \rightarrow 4'$	-0.153
$1^1B_{1g}^+$				$2 \rightarrow 2', 4 \rightarrow 1'$	0.134
	$3 \rightarrow 1'$	0.628	$1^3B_{1g}^+$	$3 \rightarrow 1'$	0.609
	$1 \rightarrow 3'$	0.637		$1 \rightarrow 3'$	0.603
				$1 \rightarrow 1', 1 \rightarrow 2'$	-0.142
$3^1A_g^-$				$1 \rightarrow 1', 2 \rightarrow 1'$	-0.251
	$1 \rightarrow 4'$	-0.341	$2^3A_g^-$	$1 \rightarrow 4'$	-0.287
	$4 \rightarrow 1'$	0.475		$4 \rightarrow 1'$	0.399
	$2 \rightarrow 3'$	-0.169		$2 \rightarrow 3'$	0.337
	$3 \rightarrow 2'$	0.128		$3 \rightarrow 2'$	-0.312
	$(1)^2 \rightarrow (1')^2$	0.315		$1 \rightarrow 2', 2 \rightarrow 1'$	-0.344
	$1 \rightarrow 2', 2 \rightarrow 1'$	0.278		$2 \rightarrow 1', 1 \rightarrow 2'$	-0.297
	$1 \rightarrow 1', 2 \rightarrow 2'$	-0.222		$5 \rightarrow 3'$	0.223
				$3 \rightarrow 5'$	-0.162
	$1 \rightarrow 1', 3 \rightarrow 3'$	-0.214			
$2^1B_{3u}^-$	$1 \rightarrow 5'$	-0.235			
	$5 \rightarrow 1'$	0.440			
	$1 \rightarrow 1', 1 \rightarrow 3'$	0.343			
	$1 \rightarrow 1', 3 \rightarrow 1'$	-0.364			
	$3 \rightarrow 4'$	-0.189			
	$4 \rightarrow 3'$	0.250			

TABLE I. (Continued)

Singlet			Triplet		
State	Transitions	Coefficients	State	Transitions	Coefficients
$3\ ^1B_{2u}^+$	$3\rightarrow 3'$	0.810	$1\ ^3A_g^+$	$2\rightarrow 3'$	0.618
	$2\rightarrow 2'$	-0.221		$3\rightarrow 2'$	0.641
	$1\rightarrow 1', 2\rightarrow 3'$	0.165		$1\rightarrow 4'$	-0.154
	$1\rightarrow 1', 3\rightarrow 2'$	0.158		$4\rightarrow 1'$	-0.128
$2\ ^3B_{1g}^-$			$2\ ^3B_{1g}^-$	$2\rightarrow 4'$	-0.423
				$4\rightarrow 2'$	0.562
				$1\rightarrow 1', 1\rightarrow 2'$	-0.238
				$1\rightarrow 1', 2\rightarrow 1'$	0.227
				$2\rightarrow 2', 1\rightarrow 2'$	0.170
				$2\rightarrow 2', 2\rightarrow 1'$	-0.188

^aThe ten valence π orbitals in naphthalene are in the order of energy: $1b_{1u}, 1b_{2g}, 1b_{3g}, 2b_{1u}, 1a_u, 2b_{2g}, 2b_{3g}, 3b_{1u}, 2a_u$, and $3b_{3g}$. The first five are occupied orbitals. They are designated by 5, 4, 3, 2, 1, 1', 2', 3', 4', and 5', respectively.

from 2 to 3' with its alternancy symmetry conjugate give the lowest $^3A_g^-$ state. Different from the corresponding singlet state, a double excitation of $(1)^2\rightarrow(1')^2$ is prohibited from the spin symmetry and the lowest $^3A_g^-$ state is expected to be dominated by the singly excited configurations. Two single excitations of $1\rightarrow 3'$ and $3\rightarrow 1'$ give rise to a pair of ionic $^3B_{1g}^-$ and covalent $^3B_{1g}^+$ states. Double excitations of $(1)^2\rightarrow(1')(2')$ with its alternancy symmetry conjugate give also $^3B_{1g}^-$ and $^3B_{1g}^+$ states in this energy range.

A. Singlet $\pi\rightarrow\pi^*$ excited states of naphthalene

We observe in Table II that CASSCF tends to overestimate the excitation energies compared to the experimental ones. Figure 3 shows that the largest errors are found in the states with the ionic *plus* character. For covalent *minus* states, the CASSCF excitation energies are still too high compared to the experiment but the deviation is much smaller than that for the ionic states. MRMP theory corrects the deficiency and represents a great improvement over CASSCF.

The lowest singlet excited state is computed to be the $^1B_{3u}^-$. Table I shows that the $^1B_{3u}^-$ state is well described by singly excited $\pi\rightarrow\pi^*$ configurations of $1\rightarrow 2'$ and $2\rightarrow 1'$, which have nearly the same weight with a different sign. The pairing property is fully satisfied at the CASSCF level. MRMP predicts it appears at 4.09 eV which shows a good agreement with the experimental value of 4.0 eV, observed in the gas-phase energy-loss spectrum.²⁴ The vapor absorption spectrum gives the peak at 3.97 eV.²¹ The $^1B_{3u}^-$ is a covalent *minus* state and the transition from the ground state of $^1A_g^-$ is pseudoparity forbidden. Transition to the $^1B_{3u}^-$ is observed to be very weak with the oscillator strength of 0.002.²¹ It is discussed that the transition to this state is vi-

bronically allowed via the b_{1g} vibration.^{27,31} The computed oscillator strength of 0.0002 is very low as expected. CASPT2 predicted the $^1B_{3u}^-$ state appears at 4.03 eV, which is very close to the present value. The SAC-CI computed the excitation energy to be 4.90 eV, which is too large compared to the experiment.

The second valence excited state was identified to be the $^1B_{2u}^+$ state. The state was predicted to locate at 4.62 eV at the MRMP level with a medium intensity of 0.0616. This is also very close to the observed peak at 4.45 eV in the absorption spectrum with the oscillator strength of 0.102.²¹ The energy-loss spectrum shows the second band in the range of 4.4–5.4 eV with the maximum at 4.7 eV.²⁴ The state comes mainly from the HOMO \rightarrow LUMO ($1\rightarrow 1'$) excitation but also contains $2\rightarrow 2'$ transition. The $^1B_{2u}^+$ state is an ionic state. Previous studies^{11,12} showed that the excitation energy of an ionic state is overestimated considerably at the CASSCF level and the introduction of a dynamic $\sigma-\pi$ polarization effect through the second-order perturbation reduces the excitation energy drastically. The transition energy to the $^1B_{2u}^+$ state is estimated to be 6.61 eV at the CASSCF level. CASSCF overestimates its energy as much as 1.9 eV. CASPT2 also gave the similar trend and predicted the transition energy to be 4.56 eV, which is also very close to the present result. Nakatsuji *et al.*⁴¹ pointed out that the dynamic σ -electron polarization is important to describe the $^1B_{2u}^+$ state. The SAC-CI, however, predicted the state lies at 5.42 eV, which is too high compared to the experiment.

The third valence excited state is the $^1B_{3u}^+$ state due to the strong optically allowed transition of $1\rightarrow 2'$ and its conjugate, which have the nearly same weight with a same sign in the CASSCF wave function. This state is also an ionic

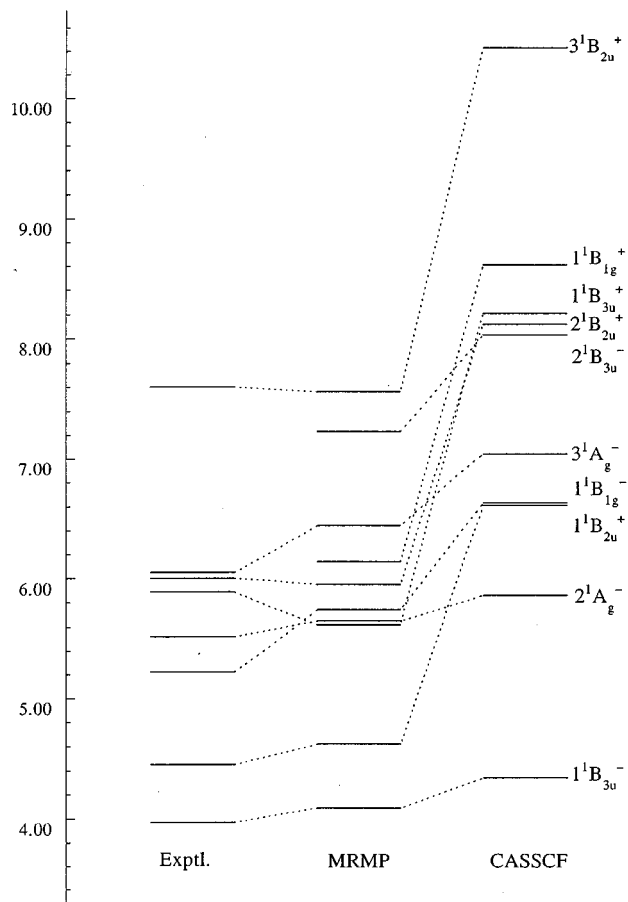
TABLE II. Valence $\pi-\pi^*$ excitation energies (eV) and oscillator strength of naphthalene.

State	Excitation energy (eV)			Oscillator strength	
	CASSCF	MRMP	Exptl.	Calculated	Exptl.
Singlet					
1 $^1B_{3u}^-$	4.34	4.09	3.97, ^a 4.0 ^b	0.0002	0.002 ^a
1 $^1B_{2u}^+$	6.61	4.62	4.45, ^{a,b} 4.7 ^c	0.0616	0.102, ^a 0.109 ^b
1 $^1B_{3u}^+$	8.21	5.62	5.89 ^{a,b,e}	1.3256	1.2, ^c 1.3 ^{a,b}
2 $^1A_g^-$	5.86	5.65	5.52 ^d	0.0000	Forbidden
1 $^1B_{1g}^-$	6.63	5.74	5.22 ^d	0.0000	Forbidden
2 $^1B_{2u}^+$	8.12	5.95	6.0 ^b	0.2678	
1 $^1B_{1g}^+$	8.61	6.14		0.0000	Forbidden
3 $^1A_g^-$	7.04	6.44	6.05 ^d	0.0000	Forbidden
2 $^1B_{3u}^-$	8.03	7.23		0.0671	
3 $^1B_{2u}^+$	10.43	7.56	7.6 ^b	0.8398	0.8 ^f
Triplet					
1 $^3B_{2u}^-$	3.16	3.15	2.98, ^g 3.0 ^h		
1 $^3B_{3u}^-$	4.35	3.95	3.82, ⁱ 3.87 ^g		
1 $^3B_{1g}^-$	4.45	4.37			
2 $^3B_{2u}^-$	4.65	4.40			
1 $^3B_{3u}^+$	6.46	4.58			
1 $^3A_g^-$	5.55	5.27			
1 $^3B_{1g}^+$	8.18	5.86			
1 $^3A_g^+$	8.13	6.07			
2 $^3A_g^-$	6.51	6.13			
2 $^3B_{1g}^-$	6.72	6.40			

^aG. A. George and G. C. Morris, J. Mol. Spectrosc. **26**, 67 (1968).^bR. H. Hubner, S. R. Mielczarek, and C. E. Kuyatt, Chem. Phys. Lett. **16**, 464 (1972).^cJ. W. McConey, S. Trajmar, K. F. Man, and J. M. Ratliff, J. Phys. B **25**, 2197 (1992).^dB. Dick and G. Hohlneicher, Chem. Phys. Lett. **84**, 471 (1981).^eT. Kitagawa, J. Mol. Spectrosc. **26**, 1 (1968).^fD. E. Mann, J. R. Platt, and H. B. Kleven, J. Chem. Phys. **17**, 481 (1949).^gP. S. Swider, M. Michaud, G. Hohlneicher, and L. Sanche, Chem. Phys. Lett. **175**, 667 (1990).^hM. Allan, J. Electron Spectrosc. **48**, 219 (1989).ⁱD. M. Hanson and G. W. Robinson, J. Chem. Phys. **43**, 4174 (1965).

state and CASSCF significantly overestimates the transition energy. The CASSCF excitation energy of 8.21 eV is reduced to 5.62 eV by the addition of the dynamic $\sigma-\pi$ polarization effect through MRMP. The oscillator strength is computed to be 1.3256, which is the strongest of all the transitions in naphthalene treated here. This transition corresponds to the most important peak of naphthalene. The absorption spectrum give the maximum peak at 5.89 eV with the oscillator strength of 1.2²⁰ and the energy-loss spectrum also gives peak at 5.89 eV with a similar intensity.²⁴ The present theory underestimates the excitation energy by 0.27 eV. CASPT2 predicted the $^1B_{3u}^+$ state lies at 5.54 eV.

A two-photon spectrum measured in solution shows a broadband with the maximum at 5.52 eV and a shoulder at 5.22 eV.^{27,28} These peaks were assigned as $^1A_g^-$ and $^1B_{1g}^-$ from the analysis of the two-photon polarization. Theory predicted the fourth valence excited state to be the $2^1A_g^-$. The state comes mainly from the two single excitations of $2\rightarrow 3'$ and $1\rightarrow 4'$ and their conjugates but includes a large fraction of doubly excited configurations of $(\text{HOMO})^2\rightarrow(\text{LUMO})^2$ and the $(\text{HOMO})(\text{HOMO}-1)\rightarrow(\text{LUMO})(\text{LUMO}+1)$. Thus the $2^1A_g^-$ is a covalent state and has a character of multiref-

FIG. 3. Schematic summary of the calculated results of the singlet $\pi\rightarrow\pi^*$ excitation energies of naphthalene.

erence nature. Even though the pairing property is also satisfied approximately at the CASSCF level. The state was predicted to locate at 5.65 eV. The transition is dipole forbidden.

MRMP predicted that the dipole forbidden $^1B_{1g}^-$ state exists slightly above the $^1A_g^-$ state. The excitation energy to this state is computed to be 5.74 eV. This state is also a mixture of the singly excited configurations of $1\rightarrow 3'$ and its conjugate and the doubly excited configurations of $(\text{HOMO})^2\rightarrow(\text{LUMO})(\text{LUMO}+1)$ and its conjugate.

Existence of two optically forbidden states is consistent with the experiment but the ordering is reverse. CASPT2 also gave the same ordering as ours: 5.39 eV ($^1A_g^-$) and 5.53 eV ($^1B_{1g}^-$). The location of the unobserved $^1A_g^-$ and $^1B_{1g}^-$ states in naphthalene is open to dispute.

The next valence excited state is computed to be $2^1B_{2u}^+$, which occurs at 5.95 eV with the oscillator strength of 0.2678. This state is described by a singly excited configuration from the second HOMO to the second LUMO, $2\rightarrow 2'$. Thus the state has an ionic character. The absorption spectrum shows a shoulder at 6.14 eV on the high energy side of the most intense $^1B_{3u}^+$ peak.²¹ The similar shoulder was also observed in the energy-loss spectrum around 6.0 eV.²⁴ These

TABLE III. Comparison of calculated and experimental energies (eV) of naphthalene.

State	MRMP	CASPT2 ⁱ	SAC-CF ^j	CNDO/S-CI ^k	Pariser's ^l	Exptl.
Singlet						
1 ¹ B _{3u} ⁻	4.09	4.03	4.90	4.02	4.018	3.97, ^a 4.0 ^b
1 ¹ B _{2u} ⁺	4.62	4.56	5.42	4.48	4.493	4.45, ^{a,b} 4.7 ^c
1 ¹ B _{3u} ⁺	5.62	5.54		6.00	5.939	5.89 ^{a,b,e}
2 ¹ A _g ⁻	5.65	5.39		5.61	5.729	5.52 ^d
1 ¹ B _{1g} ⁻	5.74	5.53		5.37	5.985	5.22 ^d
2 ¹ B _{2u} ⁺	5.95	5.93		5.98	6.309	6.0 ^b
1 ¹ B _{1g} ⁺	6.14	5.87		6.00	5.507	
3 ¹ A _g ⁻	6.44	6.04		5.76	7.359	6.05 ^d
2 ¹ B _{3u} ⁻	7.23	7.18			8.010	
3 ¹ B _{2u} ⁺	7.56	7.16			8.182	7.6 ^b
Triplet						
1 ³ B _{2u} ⁻	3.15	3.04		2.98	2.180	2.98, ^f 3.0 ^g
1 ³ B _{3u} ⁻	3.95	3.84		3.89	3.639	3.82, ^h 3.87 ^f
1 ³ B _{1g} ⁻	4.37	4.18		4.09	3.424	
2 ³ B _{2u} ⁺	4.40	4.24		4.29	4.220	
1 ³ B _{3u} ⁺	4.58	4.40		4.57	4.018	
1 ³ A _g ⁻	5.27	5.22		5.02	4.435	
1 ³ B _{1g} ⁺	5.86	5.65		6.13	5.985	
1 ³ A _g ⁺	6.07	5.77		5.74	5.715	
2 ³ A _g ⁻	6.13	5.85			6.020	
2 ³ B _{1g} ⁻	6.40	6.18		6.19	5.526	

^aG. A. George and G. C. Morris, J. Mol. Spectrosc. **26**, 67 (1968).^bR. H. Hubner, S. R. Mielczarek, and C. E. Kuyatt, Chem. Phys. Lett. **16**, 464 (1972).^cJ. W. McConey, S. Trajmar, K. F. Man, and J. M. Ratliff, J. Phys. B **25**, 2197 (1992).^dB. Dick and G. Hohlneicher, Chem. Phys. Lett. **84**, 471 (1981).^eT. Kitagawa, J. Mol. Spectrosc. **26**, 1 (1968).^fP. Swiderek, M. Michaud, G. Hohlneicher, and L. Sanche, Chem. Phys. Lett. **175**, 667 (1990).^gM. Allan, J. Electron Spectrosc. **48**, 219 (1989).^hD. M. Hanson and G. W. Robinson, J. Chem. Phys. **43**, 4174 (1965).ⁱM. Rubio, M. Merchán, E. Ortí, and B. O. Roos, Chem. Phys. **179**, 395 (1994).^jH. Nakatsuji, M. Komori, and O. Kitao, Chem. Phys. Lett. **142**, 446 (1987).^kP. Swiderek, M. Michaud, G. Hohlneicher, and L. Sanche, Chem. Phys. Lett. **175**, 667 (1990).^lR. Pariser, J. Chem. Phys. **24**, 250 (1956).

shoulders should be assigned as the transition to the 2 ¹B_{2u}⁺ state.

The state following the 2 ¹B_{2u}⁺ is computed to be the ¹B_{1g}⁺ state. Contrary to the corresponding *minus* ¹B_{1g}⁻ state, the *plus* state is dominated by singly excited configurations of 1→3' and 3→1'. The state has an ionic character and is optically forbidden. The *plus g* state is pseudoparity forbidden even for two-photon excitation. There is no experimental evidence of this state.

A first maximum of the strong bands at 6.05 eV observed in the two-photon spectrum was characterized as ¹A_g symmetry from the measured polarization.²⁷ The theory predicted the third 3 ¹A_g⁻ state appears at 6.44 eV. The state is represented by singly excited configurations of 1→4' and 2→3' with their respective conjugates but has a considerable weight of doubly excited configurations. Note that the weight of the 1→4' and 4→1' configurations is quite different. Thus the pairing property breaks down to some extent in this state. This implies that the state has mainly a covalent character but also includes a fraction of an ionic character. Therefore, the differential dynamic σ-π polarization effect becomes rather significant. CASPT2 gave 6.04 eV for this transition.

The 2 ¹B_{3u}⁻ state is computed to lie at 7.23 eV with a medium intensity. The 2 ¹B_{3u}⁻ state is a mixture of single and

double excitations. The main singly excited configurations originate from the transitions of 1→5' and 3→4' with their conjugates but the weight of conjugate pairs is no longer equivalent as in the 3 ¹A_g⁻ state. Thus the 2 ¹B_{3u}⁻ state has both covalent and ionic nature. The CASSCF excitation energy of 8.03 eV is reduced by 0.80 eV by the addition of the dynamic σ-π polarization effect through MRMP. The oscillator strength is computed to be 0.0671, which is rather large as a pseudoparity-forbidden *minus* state. This arises also from the breakdown of the pairing property. Due to the complexity of the observed spectrum in this energy region, there is no definite assignment corresponding to this state.

The second intense band of the absorption spectrum of naphthalene appears above 7 eV with a maximum at 7.6 eV.^{17,23,24} The spectrum in this energy range shows very complex structure with many overlapping Rydberg series but the broadness and intensity of the bands suggest the existence of a valence excitation.²⁴ The present theory predicted that the 3 ¹B_{2u}⁺ state lies at 7.56 eV with the oscillator strength of 0.8398, in good agreement with the experiment. This is an ionic state, mainly described by a singly excited configuration of 3→3'. CASPT2 also suggested the transition energy to this state appears at 7.16 eV.

TABLE IV. Triplet–triplet excitation energies (eV) and oscillator strength of naphthalene.

State	Excitation energy (eV)			Oscillator strength	
	CASSCF	MRMP	Exptl.	Calculated	Exptl.
$1\ ^3B_{2u}^-$	0.00	0.00		0.0000	
$1\ ^3B_{3u}^-$	1.19	0.80		0.000	Forbidden
$1\ ^3B_{1g}^-$	1.29	1.22	1.30–1.35 ^a	5×10^{-5}	$< 2 \times 10^{-4}$ ^a
$2\ ^3B_{2u}^-$	1.49	1.25		0.0000	Forbidden
$1\ ^3B_{3u}^+$	3.30	1.43		0.0000	Forbidden
$1\ ^3A_g^-$	2.39	2.11	2.25, ^b 2.17 ^c	0.0007	
$1\ ^3B_{1g}^+$	5.02	2.71	3.12 ^d	0.0854	0.14, ^b 0.12 ^a
$1\ ^3A_g^+$	4.97	2.92		3×10^{-5}	
$2\ ^3A_g^-$	3.35	2.99	2.93 ^b	0.0014	0.002 ^a
$2\ ^3B_{1g}^-$	3.56	3.25		0.0008	

^aY. M. Meyer, R. Astier, and J. M. Leclercq, J. Chem. Phys. **56**, 801 (1972).^bH. E. Hunziker, J. Chem. Phys. **56**, 400 (1972).^cW. H. Melhuish, J. Chem. Phys. **50**, 2779 (1969).^dH. E. Hunziker, Chem. Phys. Lett. **3**, 504 (1969).

B. Triplet $\pi \rightarrow \pi^*$ excited states of naphthalene

Calculated triplet excitation energies are also listed in Table II. The triplet–triplet (T – T) spectrum is summarized in Table IV with the experimental data.^{25,29,30,33–39,43} The lowest triplet excited state is the $^3B_{2u}^-$ state, which is well established in experiment.^{40,41} Transitions from the lowest triplet $^3B_{2u}^-$ state to some of the higher triplet $^3A_g^-$ and $^3B_{1g}^-$ triplet levels are allowed. Thus the major source of experimental information about the triplet states comes from the T – T absorption spectrum. Experimental information about the higher $^3B_{3u}^-$ and $^3B_{2u}^-$ states is rather limited.

The lowest triplet $^3B_{2u}^-$ state is predicted to lie at 3.15 eV with MRMP. The energy-loss spectrum of solid naphthalene yields the transition from the lowest singlet state to the lowest triplet state at 2.98 eV³⁰ and the energy-loss spectrum in the gas-phase gives the transition at 3.0 eV.²⁹ Thus our calculation is in good agreement with these experimental values. The state is dominated by singly excited configurations of $1 \rightarrow 1'$, $2 \rightarrow 2'$, and $3 \rightarrow 3'$. The $^3B_{2u}^-$ state has a covalent nature. Thus the dynamic σ – π polarization effect is of the same order as that of the ground state. CASPT2 also predicted the $^3B_{2u}^-$ state appears at 3.04 eV, which is close to the present result.

The second lowest triplet state is the $^3B_{3u}^-$ state, which is predicted to appear at 3.95 eV. The CASSCF wave function is mainly characterized by the singly excited configurations of $1 \rightarrow 2'$ and its conjugate $2 \rightarrow 1'$. This state has also a covalent nature. A weak band was observed in the $S_0 \rightarrow T$ absorption spectrum of monocrystal at 3.82 eV.³⁵ The energy-loss spectrum in the gas-phase also give a band at 3.87 eV.³⁰ This band must originate from the transition to the $^3B_{3u}^-$ state. CASPT2 also computed the transition to the $^3B_{3u}^-$ state occurs at 3.84 eV.

MRMP predicted the third triplet state is a covalent *minus* $^3B_{1g}^-$ state, located at 1.22 eV above the lowest triplet state. The state comes mainly from the transitions of $1 \rightarrow 3'$ and its conjugate. The intensity is computed to be very weak with the oscillator strength of 5×10^{-5} since the transition *minus* $T_1 \rightarrow$ *minus* T_3 is pseudoparity forbidden. This transi-

tion has not been detected in experiment. It was predicted from the corresponding transitions observed in anthracene and tetracene⁴³ that the excitation occurs at 1.30–1.35 eV with the oscillator strength less than 2×10^{-4} . Our result is consistent with the prediction. Rubio *et al.*⁴² predicted the state lies at 1.14 eV above the lowest triplet state.

The state following the $^3B_{1g}^-$ is predicted to be the $2\ ^3B_{2u}^-$ state. The state is computed to lie at 4.40 eV above the ground state. The state is represented by singly excited configurations of $2 \rightarrow 2'$ and $1 \rightarrow 1'$. CASPT2 also predicted the state locates at 4.24 eV.

The first triplet state with an ionic character is the $^3B_{3u}^+$ state. The state is predicted to lie at 4.58 eV above the ground state. The state is dominated by singly excited configurations of $1 \rightarrow 2'$ and its conjugate. Because of the ionic nature, the position of the state is affected significantly by the dynamic σ – π polarization effect. The CASSCF excitation energy is decreased by 1.88 eV at the MRMP level. The transition energy computed with CASPT2 was 4.40 eV.

As expected, the two single excitations of $2 \rightarrow 3'$ and $3 \rightarrow 2'$ result in a pair of covalent $^3A_g^-$ and ionic $^3A_g^+$ states. Contrary to the corresponding singlet states, the triplet $^3A_g^-$ and $^3A_g^+$ states are dominated by singly excited configurations since a low-lying double excitation of $(1)^2 \rightarrow (1')^2$ is prohibited from the spin symmetry. The CASSCF wave functions in Table I indicate that the singly excited configurations of $1 \rightarrow 4'$ and its conjugate are also important to describe the *minus* $^3A_g^-$ state. The transitions $2 \rightarrow 3'$ and $1 \rightarrow 4'$ give the almost same energy in Huckel approximation. The *minus* state is predicted to appear at 2.11 eV and the *plus* state at 2.92 eV, above the lowest triplet state. In addition, MRMP predicted another $^3A_g^-$ state exists slightly above the $^3A_g^+$ state. The second $2\ ^3A_g^-$ is computed to lie at 2.99 eV. This state is a mixture of the singly excited configurations of $1 \rightarrow 4'$ and $2 \rightarrow 3'$ with their conjugates and the doubly excited configurations of (HOMO)(HOMO–1) \rightarrow (LUMO)(LUMO+1). The computed oscillator strengths of these three transitions are 0.0007, 3×10^{-5} , and 0.0014, respectively, from the lowest up. Surprisingly the intensity of the

pseudoparity allowed transition to the ${}^3A_g^+$ is computed to be very weak. This is due to the fact that the ${}^3A_g^+$ and the lowest ${}^3B_{2u}^-$ states are mainly dominated by the $2 \rightarrow 3'$ and $1 \rightarrow 1'$ transitions, respectively. Thus the transition moment between these two states is zero to the first-order approximation. It was suggested the band at 2.17 eV with the oscillator strength of 0.002 in the T - T absorption spectrum is due to the ${}^3B_{2u}^- \rightarrow {}^3A_g^+$ transition.³⁶ And two peaks at 2.25 and at 2.93 eV observed in the gas-phase T - T absorption spectrum were assigned as the ${}^3A_g^-$ and ${}^3A_g^+$ states.³⁷ MRMP suggests that the band observed at 2.25 (2.17) eV is due to the first ${}^3A_g^-$ transition and the band at 2.93 eV is due to the second ${}^3A_g^-$ transition. The transition to the ${}^3A_g^+$ is very weak and probably cannot be detected in the T - T absorption spectrum. Similar results were reported by Rubio *et al.*⁴²

The strongest transition is that from the lowest triplet state to the ${}^3B_{1g}^+$.^{25,38} The band for this transition was placed at 3.12 eV with an oscillator strength of 0.14 in the T - T absorption spectrum in the gas phase.³⁹ The present theory predicted the transition occurs at 2.71 eV with the oscillator strength of 0.0854. The state has an ionic nature and is described mainly by singly excited configurations of $1 \rightarrow 3'$ and $3 \rightarrow 1'$ with a mixture of double excitations of $(\text{HOMO})^2 \rightarrow (\text{LUMO})(\text{LUMO}+1)$ and its conjugate. Due to the ionic nature, CASSCF overestimates its energy as much as 2.3 eV. CASPT2 predicted the state lies at 2.61 eV above the lowest triplet state.

Above the second ${}^3A_g^-$ state, theory predicted the existence of the second ${}^3B_{1g}^-$ state. The ${}^3B_{1g}^-$ state is a mixture of single and double excitations. The main singly excited configurations originate from the transitions of $2 \rightarrow 4'$ and $4 \rightarrow 2'$ but the weight of two configurations is no longer equivalent. Thus the state has both covalent and ionic nature. The excitation energy from the lowest triplet state was computed to be 3.25 eV at the MRMP level. The oscillator strength to this transition is computed to be 0.0008. There is no definite assignment corresponding to this state.

The present theory satisfactorily describes the ordering of all valence excited states up to 7–8 eV. The relative order of the lowest singlet u states of naphthalene is

$$\begin{aligned} 1\ {}^1B_{3u}^-(12') &< 1\ {}^1B_{2u}^+(11', 22') \\ &< 1\ {}^1B_{3u}^+(12') \\ &< 2\ {}^1B_{2u}^+(22', 33', 11') \\ &< 2\ {}^1B_{3u}^-(15', 34', 111'3') \\ &< 3\ {}^1B_{2u}^+(33', 22'). \end{aligned}$$

Main configurations are given in parentheses. We also used the abbreviation (ij') to represent the one-electron transitions of $i \rightarrow j'$ and its conjugate $j \rightarrow i'$ and $(ijk'l')$ the two-electron transitions of $(i)(j) \rightarrow (k')(l')$ and its conjugate. The relative order of the g states is

$$\begin{aligned} 2\ {}^1A_g^-(23', 111'1', 121'2') &< 1\ {}^1B_{1g}^-(13', 111'2') \\ &< 1\ {}^1B_{1g}^+(13') \\ &< 3\ {}^1A_g^-(14', 111'1', 121'2'). \end{aligned}$$

The resulting ordering for triplet u states is

$$\begin{aligned} 1\ {}^3B_{2u}^-(11', 22', 33') &< 1\ {}^3B_{3u}^-(12') \\ &< 2\ {}^3B_{2u}^-(22', 11') \\ &< 1\ {}^3B_{3u}^+(12') \end{aligned}$$

and the ordering for triplet g states is

$$\begin{aligned} 1\ {}^3B_{1g}^-(13') &< 1\ {}^3A_g^-(23', 14') \\ &< 1\ {}^3B_{1g}^+(13', 111'2') \\ &< 1\ {}^3A_g^+(23') \\ &< 2\ {}^3A_g^-(14', 23', 121'2') \\ &< 2\ {}^3B_{1g}^-(24', 111'2'). \end{aligned}$$

The covalent *minus* states always give lower energy than the corresponding ionic *plus* states. This is true for triplet states.

The calculated transition energies are in good agreement with the pertinent experimental data. We were able to predict the valence excitation energies with an accuracy of 0.27 eV for singlet u states and of 0.52 eV or better for singlet g states. Our predicted triplet states provides a consistent assignment of the T - T absorption spectrum. The error of the T - T absorption position compared to the experiment is less than 0.41 eV.

The covalent *minus* states and ionic *plus* states exhibit different behavior as far as the electron correlation is concerned. The low-lying u states and g *plus* states are dominated by the single excitations but g *minus* states with the covalent nature include a large fraction of doubly excited configurations. For singlet spin states, a double excitation of $(\text{HOMO})^2 \rightarrow (\text{LUMO})^2$ strongly admixes to the wave function of the $2\ {}^1A_g^-$. Also double-excited configurations of $(\text{HOMO})^2 \rightarrow (\text{LUMO})(\text{LUMO}+1)$ and its conjugate make a significant contribution to the $1\ {}^1B_{1g}^-$ wave function. This is true for triplet states. However, the lowest ${}^3A_g^-$ state is dominated by singly excited configurations since the $(\text{HOMO})^2 \rightarrow (\text{LUMO})^2$ excitation is prohibited by spin symmetry. As known well, the Hartree–Fock method underestimates the contribution of the covalent valence bond structure in the ground and low-lying excited states. As nondynamical electron correlation is introduced, the contribution of the ionic valence bond structure decreases in favor of larger covalent valence bond structure. Thus the low-lying double excitations are expected to have a profound effect on the covalent *minus* states in the CASSCF approximation.

The excitation energy of an ionic *plus* state is overestimated considerably at the CASSCF level and the introduction of dynamic σ - π polarization effect through the second-order perturbation reduces the excitation energy drastically. For the covalent states including the ground state, some of the dynamic σ - π polarization effects cancel each other due

to the pairing properties. Thus the dynamic σ - π polarization effect on a covalent excited state is usually of the same order as that of the ground state. However, it is not the case for ionic states and the dynamic σ - π polarization effect becomes much more significant than that on a covalent ground state.

In Sec. III we have mentioned that energies of the singlet *minus* and the corresponding triplet *plus* states are the same. This is true at the CIS level. The ionic *plus* states are usually well described by singly excited configurations but the doubly excitations are rather important for covalent *minus* states. Thus the relation breaks down at the highly correlated level. The calculated excitation energies of $1^1B_{3u}^-$, $2^1A_g^-$, and $1^1B_{1g}^-$ states are 4.09, 5.65, and 5.74 eV and the corresponding triplet excitation energies are 4.58, 6.07, and 5.86 eV, respectively. The energy splitting between singlet and triplet is small for the B_{1g} . However, it is not the case for other states.

V. LOW-LYING $\pi \rightarrow \pi^*$ EXCITED STATES OF BENZENE

The excited states of benzene have been the subject of many previous theoretical and experimental investigations. The three well-known absorption bands in the uv spectrum of benzene at 4.90, 6.20, and 6.94 eV are now unambiguously assigned to transitions which lead to states of symmetry $^1B_{2u}$, $^1B_{1u}$, and $^1E_{1u}$, respectively.^{44,45} The valence excited state of $^1E_{2g}$ has recently been observed in $S_1 \rightarrow S_n$ absorption and is located at 7.80 eV.⁴⁶

Excited states of benzene have been studied with a variety of theoretical approaches since the early days of quantum chemistry. It was rather difficult to describe the excited states of benzene accurately with *ab initio* methods. It took a long time for theoretical chemistry to achieve an accuracy less than 1 eV. Recent theoretical studies based on multireference CI with doubles (MRDCI)⁴⁷ and SAC-CI⁴⁸ computed the valence $\pi \rightarrow \pi^*$ excited states of benzene with an accuracy of about 0.5 eV. Very recent CASPT2⁴⁹ and our MRMP¹¹ also predicted the excited states with an accuracy of about 0.2 eV. In the previous paper¹¹ we have applied the state-specific MRMP to the study of valence and Rydberg excitation energies of benzene. The results compare well with the experiment. The calculated valence $\pi \rightarrow \pi^*$ excitation energies (experimental values in parentheses) are $^1B_{2u}$, 4.77 (4.90), $^1B_{1u}$, 6.28 (6.20), $^1E_{1u}$, 6.98 (6.94), and $^1E_{2g}$, 7.88 (7.80) eV, respectively. The Rydberg excitation energies are also predicted with an accuracy of 0.18 eV or better. However, the same orbitals optimized for each singlet excited state were used to compute the corresponding triplet state, which led to slightly poor description for the triplet states compared to the singlet states. The imbalance of the singlet and triplet treatment gave rise to the incorrect ordering between $^3E_{1u}$ and $^1B_{2u}$ and between $^3E_{2g}$ and $^1E_{1u}$, which are close in energy. Thus we decided to compute again the valence $\pi \rightarrow \pi^*$ excited states of benzene in refined theory with a larger basis set.

In benzene the six valence π orbitals are in the order of energy: $a_{2u}(1b_{1u})$, $e_{1g}(1b_{2g})$, $e_{1g}(1b_{3g})$, $e_{2u}(2b_{1u})$,

$e_{2u}(1a_u)$, and $b_{2g}(2b_{3g})$ in D_{6h} symmetry. The symmetry class in D_{2h} symmetry was given in parentheses. The first three are occupied orbitals. They are designated by 3, 2, 1, 1', 2', and 3', respectively. The 1 and 2 are degenerate HOMO and 1' and 2' are degenerate LUMO. The numbering of the degenerate orbitals follows Coulson's analytical solutions. The two HOMO-LUMO ($1 \rightarrow 1'$ and $2 \rightarrow 2'$) excitations give rise to the lowest $^1B_{1u}^+(^1B_{2u}^+)$ and $^1E_{1u}^+(^1B_{2u}^+)$ states. The alternant HOMO-LUMO excitations of $1 \rightarrow 2'$ and $2 \rightarrow 1'$ result in a pair of $^1B_{2u}^-(^1B_{3u}^-)$ and $^1E_{1u}^-(^1B_{3u}^-)$ states. Transitions from 1 to 3' and from 2 to 3' with their respective conjugates give degenerate $^1E_{2g}^-(^1A_g^-, ^1B_{1g}^-)$ states. Double excitations of (HOMO)² \rightarrow (LUMO)² also give rise to $^1E_{2g}^-(^1A_g^-, ^1B_{1g}^-)$ states, which lie in this energy range. Thus the strong admixture of double excitations to the wavefunction of the covalent $^1E_{2g}$ states of benzene is expected. Transitions to $^1E_{1u}^+$ states are dipole allowed while transitions to $^1B_{1u}^+$, $^1B_{2u}^+$, and $^1E_{2g}$ states are forbidden.

The main configurations of CASSCF wave functions of benzene are listed in Table V. Calculated excitation energies and oscillator strengths were summarized in Tables VI and VII. The ground state energies at the MRMP level with 6 active π orbitals and 12 active π orbitals are -231.630 73 and -231.629 03 a.u., respectively. The MRMP based on CASSCF with smaller active space gives lower energy although the energy difference is small. In general, the second-order perturbation theory tends to overestimate the correlation energy when the zeroth order Hamiltonian is not fully appropriate.

A. Singlet $\pi \rightarrow \pi^*$ excited states of benzene

First we will discuss MRMP results with the smaller 6 active π orbitals given in Table VI. The lowest singlet $\pi \rightarrow \pi^*$ excited state was computed to be the $^1B_{2u}^-(^1B_{3u}^-)$. Table V shows that the $^1B_{2u}^-$ state is mainly described by HOMO \rightarrow LUMO configurations of $1 \rightarrow 2'$ and $2 \rightarrow 1'$ but also includes a considerable amount of doubly excited configurations. MRMP predicts it appears at 4.71 eV which shows a good agreement with the experimental value of 4.90 eV. The state has a covalent nature and the σ - π polarization effect is almost similar to that in the ground state.

Second $\pi \rightarrow \pi^*$ excited states of benzene is the $^1B_{1u}^+(^1B_{2u}^+)$. The state is dominated by singly excited configurations arising from degenerate HOMO \rightarrow LUMO excitations of $1 \rightarrow 1'$ and $2 \rightarrow 2'$. Thus the state has an ionic nature. The excitation energy calculated at the CASSCF level is 7.91 eV. The introduction of the σ - π polarization effect reduces the excitation energy dramatically. The transition energy computed at the MRMP level is 5.83 eV. However, it underestimates the observed value of 6.20 eV by 0.37 eV, which implies that perturbation theory seems to overestimate the differential σ - π polarization effect considerably.

Third valence excited state is the $^1E_{1u}^+(^1B_{3u}^+, 2^1B_{2u}^+)$ state. This is the *plus* state corresponding to the *minus* $^1B_{2u}^-(^1B_{3u}^-)$ state. The CASSCF wave function of the $^1E_{1u}^+(^1B_{3u}^+)$ is dominated by the singly excited configurations of $1 \rightarrow 2'$ and $2 \rightarrow 1'$, which is different from the *minus* $^1B_{2u}^-(^1B_{3u}^-)$ state. The $^1E_{1u}^+(2^1B_{2u}^+)$ state is dominated by

TABLE V. Main configurations in CASSCF (with six active π orbitals) wave functions of benzene.^a

Singlet			Triplet		
State	Transitions	Coefficients	State	Transitions	Coefficients
$1^1A_{1g}^-(1^1A_g^-)$	$(3)^2(2)^2(1)^2$	0.943	$1^3B_{2u}^+(1^3B_{3u}^+)$	$1 \rightarrow 2'$	0.645
	$1 \rightarrow 1', 2 \rightarrow 2'$	-0.176		$2 \rightarrow 1'$	0.645
	$(1)^2 \rightarrow (1')^2$	-0.145		$1 \rightarrow 1', 2 \rightarrow 3'$	0.189
	$(2)^2 \rightarrow (2')^2$	-0.145		$1 \rightarrow 1', 3 \rightarrow 2'$	0.164
$1^1B_{2u}^-(1^1B_{3u}^-)$	$1 \rightarrow 2'$	0.632	$1^3B_{1u}^-(1^3B_{2u}^-)$	$1 \rightarrow 1'$	0.660
	$2 \rightarrow 1'$	-0.632		$2 \rightarrow 2'$	-0.660
	$1 \rightarrow 1', 2 \rightarrow 3'$	-0.168		$3 \rightarrow 3'$	-0.194
	$1 \rightarrow 1', 3 \rightarrow 2'$	0.189	$1^3E_{1u}^-(1^3B_{3u}^-)$	$1 \rightarrow 2'$	0.699
	$2 \rightarrow 2', 2 \rightarrow 3'$	-0.138		$2 \rightarrow 1'$	-0.699
	$2 \rightarrow 2', 3 \rightarrow 2'$	0.154	$1^3E_{1u}^-(2^3B_{2u}^-)$	$1 \rightarrow 1'$	0.645
$1^1B_{1u}^+(1^1B_{2u}^+)$	$1 \rightarrow 1'$	0.688		$2 \rightarrow 2'$	0.645
	$2 \rightarrow 2'$	0.688		$2 \rightarrow 2', 1 \rightarrow 3'$	0.173
$1^1E_{1u}^+(1^1B_{3u}^+)$	$1 \rightarrow 2'$	0.663		$2 \rightarrow 2', 3 \rightarrow 1'$	-0.231
	$2 \rightarrow 1'$	0.663	$1^3E_{2g}^-(1^3A_g^-)$	$1 \rightarrow 3'$	-0.461
	$1 \rightarrow 2', 1 \rightarrow 3'$	0.121		$3 \rightarrow 1'$	0.659
	$2 \rightarrow 1', 3 \rightarrow 1'$	0.148		$2 \rightarrow 1', 1 \rightarrow 2'$	0.349
$1^1E_{1u}^+(2^1B_{2u}^+)$	$1 \rightarrow 1'$	0.663		$1 \rightarrow 2', 2 \rightarrow 1'$	-0.225
	$2 \rightarrow 2'$	-0.663	$1^3E_{2g}^-(1^3B_{1g}^-)$	$2 \rightarrow 2', 1 \rightarrow 1'$	-0.268
	$2 \rightarrow 1', 2 \rightarrow 3'$	-0.121		$2 \rightarrow 3'$	-0.461
	$1 \rightarrow 2', 3 \rightarrow 2'$	-0.148		$3 \rightarrow 2'$	0.659
$1^1E_{2g}^-(2^1A_g^-)$	$1 \rightarrow 3'$	-0.361		$2 \rightarrow 2', 1 \rightarrow 2'$	0.232
	$3 \rightarrow 1'$	0.571		$2 \rightarrow 2', 2 \rightarrow 1'$	-0.261
	$(1)^2 \rightarrow (1')^2$	0.453		$1 \rightarrow 1', 1 \rightarrow 2'$	-0.261
	$1 \rightarrow 2', 2 \rightarrow 1'$	0.295		$1 \rightarrow 1', 2 \rightarrow 1'$	0.232
	$(2)' \rightarrow (1')^2$	-0.198	$1^3E_{2g}^-(1^3B_{1g}^-)$	$2 \rightarrow 3'$	-0.461
$1^1E_{2g}^-(1^1B_{1g}^-)$	$2 \rightarrow 3'$	-0.361		$3 \rightarrow 2'$	0.659
	$3 \rightarrow 2'$	0.571		$2 \rightarrow 2', 1 \rightarrow 2'$	0.232
	$2 \rightarrow 2', 1 \rightarrow 2'$	0.461		$2 \rightarrow 2', 2 \rightarrow 1'$	-0.261
	$2 \rightarrow 2', 2 \rightarrow 1'$	-0.421		$1 \rightarrow 1', 1 \rightarrow 2'$	-0.261
	$1 \rightarrow 3', 2 \rightarrow 3'$	-0.133		$1 \rightarrow 1', 2 \rightarrow 1'$	0.232
	$3 \rightarrow 1', 3 \rightarrow 2'$	0.172			

^aIn benzene the six valence π orbitals are in the order of energy: $a_{2u}(1b_{1u})$, $e_{1g}(1b_{2g})$, $e_{1g}(1b_{3g})$, $e_{2u}(2b_{1u})$, $e_{2u}(1a_u)$, and $b_{2g}(2b_{3g})$ in D_{6h} symmetry. The symmetry class in D_{2h} group was given in parentheses. The first three are occupied orbitals. They are designated by 3, 2, 1, $1'$, $2'$, and $3'$, respectively. The 1 and 2 are degenerate HOMO and $1'$ and $2'$ are degenerate LUMO.

the singly excited configurations of $1 \rightarrow 1'$ and $2 \rightarrow 2'$. The state is also ionic and the σ - π polarization effect is significant. The MRMP excitation energy is computed to be 6.33 eV. The theory underestimates the experimental value of 6.94 eV by 0.61 eV. The transition to this state is dipole-allowed and the calculated oscillator strength is 0.7558 while the experimental value is 1.25.⁵⁰

The highest valence excited state treated here is the $1^1E_{2g}^-(1^1A_g^-)$. The CASSCF wave function of the $1^1E_{2g}^-(1^1A_g^-)$ is a mixture of configurations $1 \rightarrow 3'$ and $3 \rightarrow 1'$

but includes a large fraction of the doubly excited configurations $(1)^2 \rightarrow (1')^2$, $1 \rightarrow 2'$, $2 \rightarrow 1'$, \dots etc. The absolute weights of $1 \rightarrow 3'$ and $3 \rightarrow 1'$ are no more equivalent, implying that the state is basically of covalent character but also includes an ionic nature. The $1^1E_{2g}^-(1^1B_{1g}^-)$ is also represented by a mixture of configurations $2 \rightarrow 3'$ and $3 \rightarrow 2'$ and the doubly excited configurations. Theory predicted it lies at 7.73 eV above the ground state, which is very close to the observed value of 7.80 eV.

From the MRMP results with six active π orbitals, we

TABLE VI. Valence $\pi-\pi^*$ excitation energies (eV) and oscillator strength of benzene with six active π orbitals.

State		Excitation energy (eV)			Oscillator strength	
D_{6h}	D_{2h}	CASSCF	MRMP	Exptl.	Calculated	Exptl.
Singlet						
$1^1B_{2u}^-$	$1^1B_{3u}^-$	4.82	4.71	4.90 ^a	0.0000	
$1^1B_{1u}^+$	$1^1B_{2u}^+$	7.91	5.83	6.20 ^{a,b}	0.0000	
$1^1E_{1u}^+$	$1^1B_{3u}^+$	9.29	6.33	6.94 ^a	0.7558	1.25 ^f
	$2^1B_{2u}^+$	9.29	6.33		0.7558	
$1^1E_{2g}^-$	$2^1A_g^-$	8.01	7.73	7.80 ^c	0.0000	Forbidden
	$1^1B_{1g}^-$	8.01	7.74		0.0000	
Triplet						
$1^3B_{1u}^-$	$1^3B_{2u}^-$	3.69	3.90	3.95 ^d		
$1^3E_{1u}^-$	$1^3B_{3u}^-$	4.80	4.44	4.76 ^d		
	$2^3B_{2u}^-$	4.80	4.44			
$1^3B_{2u}^+$	$1^3B_{3u}^+$	7.24	5.07	5.60 ^d		
$1^3E_{2g}^-$	$1^3A_g^-$	7.01	6.96	6.83 ^e		
	$1^3B_{1g}^-$	7.01	6.96			

^aA. Hiraya and K. Shobatake, J. Chem. Phys. **94**, 7700 (1991).^bE. N. Lassetre, A. Skerbele, M. A. Dillon, and K. J. Ross, J. Chem. Phys. **48**, 5066 (1968).^cN. Nakashima, H. Inoue, M. Sumitani, and K. Yoshihara, J. Chem. Phys. **73**, 5976 (1980).^dJ. P. Doering, J. Chem. Phys. **51**, 2866 (1969).^eR. Astier and Y. H. Meyer, Chem. Phys. Lett. **3**, 399 (1969).^fM. W. Williams, R. A. MacRae, R. N. Hamm, and E. T. Arakawa, Phys. Rev. Lett. **22**, 1088 (1969).

can see that the computational error of the ionic states, $1^1B_{1u}^+(1^1B_{2u}^+)$ and $1^1E_{1u}^+(1^1B_{3u}^+, 1^1B_{2u}^+)$, is much larger than that of the covalent states, $1^1B_{2u}^-(1^1B_{3u}^-)$ and $1^1E_{2g}^-(1^1A_g^-, 1^1B_{1g}^-)$. For the ionic states, the dynamical correlation including the $\sigma-\pi$ polarization effect is rather significant. It may be too large to be treated as a perturbation if the active space of the CASSCF theory is not large enough. So we doubled the active space in each symmetry and performed the similar calculations.

The calculated results with the 12 active π orbitals are summarized in Table VII. The enlargement of the active space has improved agreement with experiment considerably. The size of the active space has a significant effect particularly on the description of the ionic states. While the CASSCF excitation energies of the covalent states are rather insensitive to the extension of the active space, the transition energies of the ionic states has been decreased by 0.3–0.5 eV at the extended CASSCF level, which are still too high com-

TABLE VII. Valence $\pi-\pi^*$ excitation energies (eV) and oscillator strength of benzene with 12 active π orbitals.

State		Excitation energy (eV)			Oscillator strength	
D_{6h}	D_{2h}	CASSCF	MRMP	Exptl.	Calculated	Exptl.
Singlet						
$1^1B_{2u}^-$	$1^1B_{3u}^-$	4.89	4.67	4.90 ^a	0.0000	
$1^1B_{1u}^+$	$1^1B_{2u}^+$	7.57	6.14	6.20 ^{a,b}	0.0000	
$1^1E_{1u}^+$	$1^1B_{3u}^+$	8.78	6.84	6.94 ^a	0.8599	1.25 ^f
	$2^1B_{2u}^+$	8.78	6.84		0.8599	
$1^1E_{2g}^-$	$2^1A_g^-$	8.04	7.71	7.80 ^c	0.0000	Forbidden
	$1^1B_{1g}^-$	8.04	7.71		0.0000	
Triplet						
$1^3B_{1u}^-$	$1^3B_{2u}^-$	3.85	3.83	3.95 ^d		
$1^3E_{1u}^-$	$1^3B_{3u}^-$	4.83	4.47	4.76 ^d		
	$2^3B_{2u}^-$	4.83				
$1^3B_{2u}^+$	$1^3B_{3u}^+$	6.78	5.45	5.60 ^d		
$1^3E_{2g}^-$	$1^3A_g^-$	7.15	6.92	6.83 ^e		
	$1^3B_{1g}^-$	7.15	6.92			

^aA. Hiraya and K. Shobatake, J. Chem. Phys. **94**, 7700 (1991).^bE. N. Lassetre, A. Skerbele, M. A. Dillon, and K. J. Ross, J. Chem. Phys. **48**, 5066 (1968).^cN. Nakashima, H. Inoue, M. Sumitani, and K. Yoshihara, J. Chem. Phys. **73**, 5976 (1980).^dJ. P. Doering, J. Chem. Phys. **51**, 2866 (1969).^eR. Astier and Y. H. Meyer, Chem. Phys. Lett. **3**, 399 (1969).^fM. W. Williams, R. A. MacRae, R. N. Hamm, and E. T. Arakawa, Phys. Rev. Lett. **22**, 1088 (1969).

pared to the experiment. The MRMP results with 12 active π orbitals represent a great improvement for the ionic states over those with 6 active π orbitals. The oscillator strength of the dipole allowed ${}^1E_{1u}^+$ transition is also improved. The deviation of the excitation energy from the experiment is within 0.23 eV for all the singlet states. The present calculations lead to the conclusion that the accurate description of the ionic states needs large enough active space.

B. Triplet $\pi \rightarrow \pi^*$ excited states of benzene

The lowest three triplet states of benzene were observed at 3.95, 4.76, and 5.60 eV by the low-energy electron impact study.⁵¹ These are assigned as ${}^3B_{1u}$ and ${}^3E_{1u}$, and ${}^3B_{2u}$, respectively. The fourth valence triplet state of ${}^3E_{2g}$ was determined to lie at 6.83 eV from the T-T absorption spectrum.⁵²

For triplet states, the two HOMO-LUMO ($1 \rightarrow 1'$ and $2 \rightarrow 2'$) excitations give rise to the lowest ${}^3B_{1u}^-({}^3B_{2u}^-)$ and ${}^3E_{1u}^-({}^3B_{2u}^-)$ states. The alternant HOMO-LUMO excitations of $1 \rightarrow 2'$ and $2 \rightarrow 1'$ result in a pair of ${}^3E_{1u}^-({}^3B_{3u}^-)$ and ${}^3B_{2u}^+({}^3B_{3u}^+)$ states. Transitions from 1 to $3'$ and from 2 to $3'$ with their alternancy symmetry conjugates give degenerate ${}^3E_{2g}^-({}^3A_g^-, {}^3B_{1g}^-)$ states. The doubly excited triplet states arising from the transitions such as $1 \rightarrow 1'$, $2 \rightarrow 2'$ and $1 \rightarrow 2'$, $2 \rightarrow 1'$ exist in lower energy region and are expected to interact with the singly excited states of ${}^3E_{2g}^-$. In the case of naphthalene, the ${}^3A_g^-$ state is dominated by singly excited configurations and we cannot see any mixture of doubly excited configurations. In benzene, however, the occupied 1 and 2 and unoccupied $1'$ and $2'$ are degenerate and the ${}^3E_{2g}^-({}^3A_g^-, {}^3B_{1g}^-)$ states are expected to have a considerable fraction of doubly excited configurations. Thus, the situation is different from that in naphthalene.

The calculated triplet excitation energies are summarized in Table VI. The lowest triplet excited states of benzene is the ${}^3B_{1u}^-({}^3B_{2u}^-)$. The state is dominated by singly excited configurations arising from HOMO-LUMO excitations of $1 \rightarrow 1'$ and $2 \rightarrow 2'$. The state has a covalent nature. The transition energy computed at the MRMP level is 3.90 eV, which is in good agreement with the observed value of 3.95 eV.

Second valence triplet excited state is the ${}^3E_{1u}^-({}^3B_{3u}^-, {}^3B_{2u}^-)$ state. The CASSCF wave function of the ${}^3E_{1u}^-({}^3B_{3u}^-)$ is dominated by the singly excited configurations of $1 \rightarrow 2'$ and $2 \rightarrow 1'$. However, the ${}^3E_{1u}^-({}^3B_{2u}^-)$ state is represented by a mixture of singly and doubly excitations. The state is also of covalent nature. The MRMP excitation energy is computed to be 4.44 eV, which is smaller by 0.32 eV compared to the experimental value of 4.76 eV.

Third lowest triplet excited state is computed to be the ${}^3B_{2u}^+({}^3B_{3u}^+)$. This is the *plus* state corresponding to the *minus* ${}^3E_{1u}^-({}^3B_{3u}^-)$. The ${}^3B_{2u}^+({}^3B_{3u}^+)$ state is mainly described by singly excited configurations of $1 \rightarrow 2'$ and $2 \rightarrow 1'$ but also includes a considerable amount of doubly excited configurations. MRMP predicts it appears at 5.07 eV. The deviation from the experiment is as much as 0.53 eV. This indicates also that the MRMP based on the smaller CASSCF is rather poor for the description of a triplet ionic state.

The highest valence excited state treated here is the ${}^3E_{2g}^-({}^3A_g^-, {}^3B_{1g}^-)$. The CASSCF wave function of the ${}^3E_{2g}^-({}^3A_g^-)$ is a mixture of singly excited configurations $1 \rightarrow 3'$ and $3 \rightarrow 1'$ and the doubly excited configurations. Similar to the corresponding singlet state, the triplet state is a mixture of covalent and ionic character. The present theory predicted it lies at 6.96 eV above the ground state, which is very close to the observed value of 6.83 eV.

The MRMP results with 12 active π orbitals given in Table VII show a great improvement for the ionic states over the MRMP with 6 active π orbitals. The extension of the active space has also a significant effect on the description of the ionic states. The maximum deviation from the experiment is 0.29 eV for the case of the ${}^3E_{1u}^-$ state.

The present MRMP with 12 active π orbitals satisfactorily describes the low-lying valence excited states of benzene. The relative order of the lowest singlet u states of benzene is

$${}^1B_{2u}^-({}^1B_{3u}^-)(12') < {}^1B_{1u}^+({}^1B_{2u}^+)(11', 22') \\ < {}^1E_{1u}^+({}^1B_{3u}^+)(12') = {}^1E_{1u}^+({}^1B_{2u}^+)(22', 11').$$

The resulting ordering for triplet u states is

$${}^3B_{1u}^-({}^3B_{2u}^-)(11', 22') < {}^3E_{1u}^-({}^3B_{3u}^-)(12') \\ = {}^3E_{1u}^-({}^3B_{2u}^-)(22', 11') \\ < {}^3B_{2u}^+({}^3B_{3u}^+)(12').$$

The ordering is the same as that in naphthalene. The covalent *minus* states also give lower energy than the corresponding ionic *plus* states. The singlet and triplet ${}^1, {}^3E_{2g}^-({}^1, {}^3A_g^-, {}^1, {}^3B_{1g}^-)$ states are a strong mixture of singly and doubly excited configurations.

The calculated transition energies are in good agreement with the pertinent experimental data. We were able to predict the valence excitation energies with an accuracy of 0.23 eV for singlet states and of 0.29 eV or better for triplet states with MRMP based on the 12 active π orbitals.

VI. SUMMARY

Multireference perturbation theory with CASSCF reference functions was applied to the study of the valence $\pi \rightarrow \pi^*$ excited states of benzene and naphthalene. The present approach leads to the prediction of benzene and naphthalene spectra which provide a consistent assignment of the experimental data. The eigenvectors and eigenvalues of CASSCF with valence π active orbitals satisfy pairing properties for the alternant hydrocarbons to a good approximation. The excited states of polyacenes are classified into the covalent *minus* states and ionic *plus* states with the use of the alternancy symmetry. The pairing properties, which are rather approximation invariant, are proved to be valuable in interpreting the excited states of benzene and naphthalene.

The present theory satisfactorily describes the ordering of low-lying valence $\pi \rightarrow \pi^*$ excited states. The calculated transition energies are in good agreement with the pertinent experimental data although the comparison with the experi-

ment is not straightforward. We were able to predict the valence excitation energies with an accuracy of 0.27 eV for singlet u states and of 0.52 eV or better for singlet g states of naphthalene. Our predicted triplet states spectrum provides a consistent assignment of the T–T absorption spectrum of naphthalene. For benzene we are able to predict the valence excitation energy with an accuracy of about 0.29 eV.

The covalent *minus* states and ionic *plus* states exhibit different behavior as far as the electron correlation is concerned. The ionic *plus* states are dominated by the single excitations but covalent *minus* states (especially g states) include a large fraction of doubly excited configurations. For singlet spin states, a double excitation of $(\text{HOMO})^2 \rightarrow (\text{LUMO})^2$ strongly admixes to the wave functions of the 2^1A_{1g} state of naphthalene and 1^1E_{2g} state of benzene. Also doubly excited configurations of $(\text{HOMO})^2 \rightarrow (\text{LUMO})(\text{LUMO}+1)$ and its conjugate make a significant contribution to the 1^1B_{1g} of naphthalene and 1^1E_{2g} state of benzene. This is true for triplet states. However, the lowest 3^1A_{1g} state of naphthalene is dominated by a singly excited configuration since the $(\text{HOMO})^2 \rightarrow (\text{LUMO})^2$ excitation is prohibited by spin symmetry. The covalent *minus* states always give lower energy than the corresponding ionic *plus* states both for singlet and triplet states.

The excitation energies of ionic *plus* states are overestimated considerably at the CASSCF level and the introduction of dynamic σ – π polarization effects through the second-order perturbation reduces the excitation energies drastically. The dynamic σ – π polarization effects on covalent excited states are usually the same as in the covalent ground state. The enlargement of the active space of the reference functions represents a great improvement of the description of the ionic states.

In our study we had to leave unassigned a number of excitations, particularly triplet excitations in naphthalene. In this respect we hope that our calculations will stimulate further spectroscopic work.

The present approach with the pairing properties will be of great value in understanding and predicting the experimental data of the alternant hydrocarbons and even of their substituted and heterocyclic analogues.

ACKNOWLEDGMENTS

The present research is supported in part by the grant-in-aid for Scientific Research on Priority Area "Theory of Chemical Reactions" from the Ministry of Education, Science and Culture and by the grant from New Energy and Industrial Technology Development Organization (NEDO). The computations were carried out on the IBM RS6000-590 workstations at IMS. The CASSCF reference wave functions were obtained by the MOLPRO⁵³ programs. The perturbation calculations were performed with MR2D program.⁵⁴

¹E. Huckel, Z. Phys. **70**, 206 (1931); *ibid.* **72**, 310 (1931); *ibid.* **76**, 628 (1932).

²M. Goeppart-Mayer and A. L. Sklar, J. Chem. Phys. **6**, 645 (1938).

³R. Pariser and R. G. Parr, J. Chem. Phys. **21**, 466, 767 (1953).

⁴J. A. Pople, Trans. Faraday Soc. **49**, 1375 (1953).

- ⁵C. A. Coulson and G. S. Rushbrooke, Proc. Camb. Philos. Soc. **36**, 193 (1940).
- ⁶J. Koutecky, J. Chem. Phys. **44**, 3702 (1966).
- ⁷J. Cizek, J. Paldus, and I. Hubac, Int. J. Quantum Chem. **8**, 951 (1974).
- ⁸P. Tavan and K. Schulten, J. Chem. Phys. **70**, 5414 (1979).
- ⁹K. Hirao, Chem. Phys. Lett. **190**, 374 (1992); *ibid.* **196**, 397 (1992); *ibid.* **201**, 59 (1993); Intern. J. Quantum Chem. S **26**, 517 (1992).
- ¹⁰P. E. Siegbahn, A. Heiberg, B. O. Roos, and B. Levy, Phys. Scr. **21**, 323 (1980); B. O. Roos, P. R. Taylor, and P. E. Siegbahn, Chem. Phys. **48**, 157 (1980); B. O. Roos, Int. J. Quantum Chem. S **14**, 175 (1980).
- ¹¹K. Hirao, H. Nakano, and T. Hashimoto, Chem. Phys. Lett. **235**, 430 (1995).
- ¹²T. Tsuneda, H. Nakano, and K. Hirao, J. Chem. Phys. **103**, 6520 (1995); H. Nakano, T. Tsuneda, T. Hashimoto, and K. Hirao, J. Chem. Phys. **104**, 2312 (1996).
- ¹³A. Langseth and B. P. Stoicheff, Can. J. Phys. **34**, 350 (1956); K. K. Innes, J. E. Parkin, and D. K. Ervin, J. Mol. Spectrosc. **16**, 406 (1965).
- ¹⁴T. H. Dunning, J. Chem. Phys. **90**, 1007 (1989).
- ¹⁵R. Pariser, J. Chem. Phys. **24**, 250 (1956).
- ¹⁶C. A. Coulson, Proc. Phys. Soc. London, Ser. A **60**, 257 (1948).
- ¹⁷H. B. Klevens and J. R. Platt, J. Chem. Phys. **17**, 470 (1949).
- ¹⁸A. Bree and T. Thirunamachandran, Mol. Phys. **5**, 397 (1962).
- ¹⁹M. A. El-Sayed and T. Pavlopoulos, J. Chem. Phys. **39**, 834 (1963).
- ²⁰T. Kitagawa, J. Mol. Spectrosc. **26**, 1 (1968).
- ²¹G. A. George and G. C. Morris, J. Mol. Spectrosc. **26**, 67 (1968).
- ²²J. Jortner and G. C. Morris, J. Chem. Phys. **51**, 3689 (1969).
- ²³E. E. Koch, A. Otto, and K. Radler, Chem. Phys. Lett. **16**, 131 (1972).
- ²⁴R. H. Huebner, S. R. Mielczarek, and C. E. Kuyatt, Chem. Phys. Lett. **16**, 464 (1972).
- ²⁵R. Scheps, D. Florida, and S. A. Rice, J. Chem. Phys. **56**, 295 (1972).
- ²⁶N. Mikami and M. Ito, Chem. Phys. Lett. **31**, 472 (1975).
- ²⁷M. J. Robey, I. G. Ross, R. V. Southwood-Jones, and S. J. Stricker, Chem. Phys. **23**, 207 (1977).
- ²⁸B. Dick and G. Hohlneicher, Chem. Phys. Lett. **84**, 471 (1981).
- ²⁹M. Allan, J. Electron Spectrosc. Relat. Phenom. **48**, 219 (1989).
- ³⁰P. Swiderek, M. Michaud, G. Hohlneicher, and L. Sanche, Chem. Phys. Lett. **175**, 667 (1990).
- ³¹C. C. Bonang and S. M. Cameron, J. Chem. Phys. **97**, 5377 (1992).
- ³²J. W. McConey, S. Trajmar, K. F. Man, and J. M. Ratliff, J. Phys. B **25**, 2197 (1992).
- ³³G. Porter and F. G. Wright, Trans. Faraday Soc. **63**, 530 (1955).
- ³⁴C. A. Hutchison and B. W. Mangum, J. Chem. Phys. **34**, 908 (1961).
- ³⁵D. M. Hanson and G. W. Robinson, J. Chem. Phys. **43**, 4174 (1965).
- ³⁶W. H. Melhuish, J. Chem. Phys. **50**, 2779 (1969).
- ³⁷H. E. Hunziker, Chem. Phys. Lett. **3**, 504 (1969).
- ³⁸T. G. Pavlopoulos, J. Chem. Phys. **53**, 4230 (1970).
- ³⁹H. E. Hunziker, J. Chem. Phys. **56**, 400 (1972).
- ⁴⁰G. Hohlneicher and B. Dick, J. Chem. Phys. **70**, 5427 (1979).
- ⁴¹H. Nakatsuji, M. Komori, and O. Kitao, Chem. Phys. Lett. **142**, 446 (1987).
- ⁴²M. Rubio, M. Merchán, E. Ortí, and B. O. Roos, Chem. Phys. Lett. **179**, 395 (1994).
- ⁴³Y. H. Meyer, R. Astier, and J. M. Leclercq, J. Chem. Phys. **56**, 801 (1972).
- ⁴⁴E. N. Lassette, A. Skerbele, M. A. Dillon, and K. J. Ross, J. Chem. Phys. **48**, 5066 (1968).
- ⁴⁵A. Hiraya and K. Shobatake, J. Chem. Phys. **94**, 7700 (1991).
- ⁴⁶N. Nakashima, H. Inoue, M. Sumitani, and K. Yoshihara, J. Chem. Phys. **73**, 5976 (1980).
- ⁴⁷M. H. Palmer and I. C. Walker, Chem. Phys. **133**, 113 (1989).
- ⁴⁸O. Kitao and H. Nakatsuji, J. Chem. Phys. **87**, 1169 (1987).
- ⁴⁹B. O. Roos, K. Andersson, and M. P. Fulscher, Chem. Phys. Lett. **192**, 5 (1992).
- ⁵⁰M. W. Williams, R. A. MacRac, R. N. Hamm, and E. T. Arakawa, Phys. Rev. Lett. **22**, 1088 (1969).
- ⁵¹J. P. Doering, J. Chem. Phys. **51**, 2866 (1969).
- ⁵²R. Astier and Y. H. Meyer, Chem. Phys. Lett. **3**, 399 (1969).
- ⁵³MOLPRO is a package of *ab initio* programs written by H.-J. Werner and P. J. Knowles; J. Chem. Phys. **73**, 2342 (1980); Chem. Phys. Lett. **115**, 259 (1985).
- ⁵⁴H. Nakano, J. Chem. Phys. **99**, 7983 (1993); MR2D Ver.2, H. Nakano (University of Tokyo, 1995).